

⁶Yu. M. Gal'perin, V. L. Gurevich, and V. I. Kozub, Zh. Eksp. Teor. Fiz. 65, 1045 (1973) [Sov. Phys. JETP 38, 517 (1974)].

⁷A. G. Aronov and R. Katilyus, Zh. Eksp. Teor. Fiz. 68, 2208 (1975) [Sov. Phys. JETP 41, 1106 (1975)].

⁸V. L. Gurevich, Yu. M. Gal'perin, and V. I. Kozub, Zh. Eksp. Teor. Fiz. 66, 1387 (1974) [Sov. Phys. JETP 39, 680 (1974)].

Translated by D. ter Haar

Dynamics of a Z-pinch in n -InSb under impact ionization conditions

V. V. Vladimirov, V. N. Gorshkov, and M. P. Semesenko

Physics Institute, Ukrainian Academy of Sciences

(Submitted November 4, 1975)

Zh. Eksp. Teor. Fiz. 70, 1490–1500 (April 1976)

A nonstationary theory of a Z-pinch in n -InSb is developed by taking into account quadratic volume recombination and electron-hole scattering. The time scans of the electric field intensity are calculated for a sample under prescribed current conditions. It is shown that the scans are oscillatory as a result of excitation of an ionization domain in the crystal under pinch conditions. If electron-hole scattering is taken into account the oscillations can arise only in a definite current range corresponding to a strongly developed pinch. The frequency and amplitude of the oscillations are calculated as functions of current and of the recombination and scattering parameters. The pinch radius, pinch time, and shape of the current-voltage characteristics are determined. It is shown that the dependence of the pinch radius on current is nonmonotonic (possesses a minimum) under electron-hole scattering conditions. The theoretical results are compared with available experimental data, some of which are explained for the first time. Most of the calculations were carried out with a computer.

PACS numbers: 71.85.—a

1. The Z pinch phenomenon in a gas plasma wherein the plasma is compressed by the magnetic field of its own current, is well known.^[1,2] Much later, Glicksman and Steele^[3] observed this phenomenon in the electron-hole plasma of a semiconductor by investigating the anomalies of the resistance of InSb samples with electronic conductivity (n -InSb) in the impact-ionization (interband breakdown) regime at low lattice temperatures ($T_c = 77^\circ\text{K}$). It turned out that at large currents ($I > 5\text{ A}$) the plasma resistance decreased when the samples were located in a longitudinal magnetic field ($\mathbf{H} \parallel \mathbf{E}$, where \mathbf{E} is the electric field intensity at the sample) comparable in strength with magnetic field of the current (H_ϕ). Glicksman and Steele have advanced the hypothesis that the anomalous resistance of the samples, which occurs at $H=0$, is due to pinching of the plasma. When the plasma contracts its resistance increases, since the processes of quadratic volume recombination and electron-hole scattering, which decrease the number of particles^[4] and the electron mobility,^[5] become stronger. The pinch effect can become weaker and the plasma resistance can decrease in a longitudinal magnetic field. Glicksman and Steele's guess was soon confirmed^[6,7] by a series of experiments in which this phenomenon was revealed by using direct procedures for observing strong contraction of the plasma. It turned out^[8] that the destruction of the pinch in a longitudinal magnetic field is due to the development of a screw instability,^[9] which leads to an anomalous escape of plasma to the sample surface. A number of subsequent studies^[10–12] have shown that the plasma

contraction in n -InSb under given-current conditions evolves in time in a rather complicated manner. Thus, for sufficiently large current the time sweeps of the field intensity (E) at the sample have an oscillatory character. It was shown in^[10] that the frequency and damping time of these oscillations increase with the current. On the other hand, it is noted in^[11] that these oscillations appear in the current transition region to the state of strong plasma contraction. It is shown in^[12] that the pinch oscillations appear in a larger range of currents when the pinch is already developed, but the oscillations vanish at larger values of I .

It will be shown here that this phenomenon has indeed a complex character and depends strongly on the initial crystal parameters that determine directly or indirectly the role of the electron-hole scattering (impurity concentration, mobilities and lifetimes of the non-equilibrium carriers, etc.). At present there are two (theoretically justified) points of view concerning the nature of these oscillations. According to^[13] the oscillations of the field E can be due to the magnetothermal character of the pinch, when the heating of the lattice and the thermal ionization in the region of strong contraction play an essential role. In the given-current regime, periodic heating and cooling of the lattice in the pinch channel can take place, and the sample conductivity oscillates correspondingly. This concept, however, can hardly be used to explain the experiments performed with short pulses ($\tau_{\text{pulse}} \lesssim 10^{-6}\text{ sec}$) and relatively weak currents ($I < 20\text{ A}$), when the lattice is

weakly heated in the region of the pinch channel.^[7] Igitkhanov and Kadomtsev^[14] have shown that the pinch oscillations can be due to excitation of plasma instabilities of the constriction type ($m=0$). This instability was indeed observed in experiments performed on p -InSb in the injection regime,^[15] but no constrictions were observed in experiments on n -InSb in the impact-ionization regime, although the corresponding hypothesis was advanced^[12] (the spatial structure of the perturbations was not measured in^[12]). We note that in the cited theoretical papers^[13,14] no account was taken of the quadratic volume recombination, of electron-hole scattering, and of impact ionization.

It will be shown in this paper that allowance for these processes leads to an oscillatory establishment of the stationary state for the case of the pinch effect in n -InSb in the given-current regime. It turns out that the evolution of the pinch effect in the crystal consists of two regions, a central region in which recombination and scattering processes predominate (the strong contraction region) and a peripheral region where the principal role is played by impact ionization. In the case of strong plasma contraction the escape of the particles from the latter region is decreased, and a plasma-density wave (domain) is generated in the region. As this wave develops, conditions arise for its "disengagement" from the region where it is generated, and the wave begins to move into the central region. When the leading front of the ionization wave enters the strong-pinch region, a conductivity spike is produced. This process can repeat periodically and lead to oscillations of the electric field intensity. It has been shown that when account is taken of the electron-hole scattering, which weakens the pinching effect, oscillations are produced only in a definite current interval corresponding to strong contraction of the plasma.

We calculate in this paper the dependences of the frequency, amplitude, and damping coefficient of these oscillations on the current, and obtain the principal characteristics of the pinch (the dependence of the radius of the pinch channel and of the pinching time on the current, the spatial distribution of the plasma, the form of the current-voltage characteristics—CVC). The results agree well in a number of cases with the experimental data.

2. In contrast to low-pressure gas plasma, the particle inertia does not play any role in the contraction of an electron-hole plasma, since the carrier momentum relaxation times are small ($\sim 10^{-12}$ sec). The pinch effect results in this case from ambipolar drift of the electrons and holes in the longitudinal electric field and in the azimuthal magnetic field of the current. We note that in a gas plasma oscillations are due to the inertia of the heavy ions.^[16]

The initial equation of the problem, describing the change of the plasma density in space and in time in an n -type semiconductor during the pinch effect under impact-ionization conditions, can be obtained by using the equations of motion of the electrons and holes,^[17,18] the continuity equation for the radial ambipolar flux (Γ_r), and Maxwell's equation for the magnetic field due to the

current. Assuming that the nonequilibrium plasma is quasi-neutral, the skin effect is weak (the electric field is constant over the sample cross section), and that all the quantities depend only on the radius and the time, these equations take the form

$$v_{er} = -\frac{D_e}{n+n_0} \frac{\partial n}{\partial r} - b_e E_r + \frac{b_e}{c} v_{eh} H_\phi, \quad v_{eh} = -b_e E; \quad (1)$$

$$v_{hr} = -\frac{D_h}{n} \frac{\partial n}{\partial r} + b_h E_r - \frac{b_h}{c} v_{eh} H_\phi, \quad v_{eh} = b_h E; \quad (2)$$

$$\frac{\partial n}{\partial t} + \frac{1}{r} \frac{\partial (r\Gamma_r)}{\partial r} = G(n+n_0) - r'n(n+n_0); \quad (2)$$

$$H_\phi = \frac{4\pi e E}{cr} \int_0^r (b_e + b_h)(n+n_0)r dr. \quad (3)$$

Here $v_{e,h}$ are the electron and hole velocities; $D_{e,h}$ and $b_{e,h}$ are the diffusion and mobility coefficients, n is the density of the nonequilibrium carriers, n_0 is the density of the impurity electrons, E_r and $\Gamma_r = (n+n_0)v_{er} = nv_{hr}$ are the radial ambipolar electric field and the flux, G is the impact-ionization coefficient, and r' is the coefficient of the quadratic volume recombination.

In the derivation of the equations of motion we did not take into account the magnetoresistance effect due to the magnetic field of the current, since they are weakly pronounced in all the known experiments ($b_e b_h H_\phi^2 / c^2 \ll 1$). Nor were the heating of the carriers and of the lattice or the plasma degeneracy effects taken into account. As a rule, under the conditions of the pinch effect in n -InSb, the carrier heating is limited by the excitation of optical phonons and $T_e \approx T_h \approx 250$ K.^[3,6,7,10] At this temperature, the degeneracy of the electronic component sets in at $n \approx 10^{17}$ cm⁻³.

All the subsequent calculations will be carried out in the approximation $b_e \gg b_h$ (InSb), which is usually valid even if the electron-hole scattering is taken into account,^[5] when the electron mobility decreases as the plasma contracts:

$$b_e = b_{e0} / (1 + \alpha N), \quad (4)$$

where $N = n/n_0$ and b_{e0} is the electron mobility at low plasma density. An expression for the coefficient α is given in^[5,19]. In InSb, $\alpha \approx 0.01$ if $T_e = 250$ K, $b_{e0} = 7.5 \cdot 10^7$ cgs esu ($T_e = 77$ K), $n_0 = 2 \cdot 10^{14}$ cm⁻³. In this case

$$\Gamma_r = -D_h \frac{2n+n_0}{n+n_0} \frac{\partial n}{\partial r} - \frac{b_e b_h}{c} n E H_\phi, \quad (5)$$

$$E = I / 2\pi e \int_0^r b_e (n+n_0) r dr, \quad (6)$$

where R is the radius of the sample.

The shape of the current pulse was specified by us in the form

$$I(t) = I_0 (1 - e^{-t/\tau}), \quad (7)$$

where τ is the time required for the current to grow to the maximum value of I_0 ($\tau \approx 10^{-8}$ sec in many experiments^[8,10]). The dependence of the impact-ionization coefficient G on the electric field was chosen in the form

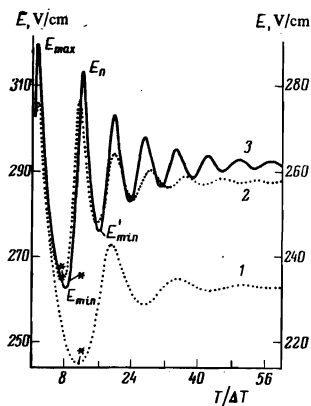


FIG. 1. Time scans of the electric field intensity at the sample ($\gamma=0.128$; $\alpha=0.01$; $R^-=2$); curves 1— $I_0=5$ A, 2— $I_0=7$ A, $\Delta T=1/160$; 3— $I_0=12$ A, $\Delta T=1/320$ (left-hand scale for curve 3, right-hand scale for 1 and 2).

$$G=g_0 e^{bE}; \quad (8)$$

here $g_0=5 \times 10^3 \text{ sec}^{-1}$ and $b=0.033 \text{ cm/V}$.

This dependence was determined experimentally in^[20] (*n*-InSb, $T=77^\circ \text{K}$). The value of the volume recombination coefficient of InSb is $r' \approx 5 \times (19^{-8} - 10^{-9}) \text{ cm}^3/\text{sec}$.

Substituting expression (5) in Eq. (2) and taking relations (3), (4), and (6)–(8) into account, we obtain the initial equation of the problem:

$$\frac{\partial N}{\partial T} - \frac{\gamma}{\rho} \frac{\partial}{\partial \rho} \left(\rho \frac{2N+1}{N+1} \frac{\partial N}{\partial \rho} \right) - \frac{\beta A^2(T)}{\sigma^2(\rho=1, T)} \frac{1}{\rho} \frac{\partial}{\partial \rho} \left(\frac{N}{1+\alpha N} \sigma(\rho, T) \right) = R^+ (1+N) \exp \left[\frac{E_0 A(T)}{\sigma(\rho=1, T)} \right] - R^- N(1+N), \quad (9)$$

where

$$\sigma(\rho, T) = 2 \int_0^{\rho} \frac{1+N}{1+\alpha N} \rho' d\rho', \quad A(T) = 1 - e^{-T/\tau}, \quad T = \frac{t}{\tau},$$

$$\rho = \frac{r}{R}, \quad \gamma = \frac{\tau_{\text{pulse}} D_n}{R^2}, \quad \beta = \frac{\tau_{\text{pulse}}}{\tau_{\text{pinch}}}, \quad \tau_a = \frac{\pi c^2 e R^2 n_0}{2 b_0 I_0^2}, \quad \tau = -\frac{r'}{\tau_{\text{pinch}}}$$

$$R^+ = g_0 \tau_{\text{pulse}}, \quad R^- = r' n_0 \tau_{\text{pulse}}, \quad E_0 = b I_0 / \pi e b_0 n_0 R^2,$$

τ_{pulse} is the duration of the current pulse. The function $\sigma(\rho=1, T)$ determines the conductivity of the sample, and $\sigma(\rho=1, \alpha=0, T)=U$ is the number of particles in the sample. The initial condition is

$$N(T=0, \rho)=0, \quad (10)$$

and the boundary condition is that the radial flux on the sample surface be equal to the surface-recombination flux:

$$\frac{2N+1}{N+1} \frac{\partial N}{\partial \rho} \Big|_{\rho=1} + \frac{\beta A^2(T) N}{(1+\alpha N) \sigma(\rho, T)} \Big|_{\rho=1} = -\bar{S} N|_{\rho=1}, \quad (11)$$

where $\bar{S} = s \tau_{\text{pulse}} / R$ and s is the rate of surface recombination. In the case of sufficiently large currents, when the pinch effect is strong, $\beta \gg \bar{S}$ ($S_{\text{pinch}}/R \ll 1$) and the recombination on the surface is negligible (the plasma resulting from impact ionization is rapidly compressed to the sample axis). We shall henceforth assume $\bar{S}=0$.

Solutions of Eqs. (9)–(11) were obtained with a com-

puter. The character of the solutions was investigated as a function of the current for different values of the parameters of ambipolar diffusion γ , volume recombination R^+ , and electron-hole scattering α . The values of β' ($\beta = \beta' I_0^2$), E'_0 ($E_0 = E' I_0$) and τ were fixed at $\beta' = 0.83 \text{ A}^{-2}$, $E'_0 = 3.28 \text{ A}^{-1}$, $\tau = 10^{-2}$. These values correspond, for example, to the following given initial parameters: $n_0 = 2 \cdot 10^{14} \text{ cm}^{-3}$, $b_n = 2 \cdot 10^6$, $b_{e0} = 7.5 \cdot 10^7 \text{ cgs esu}$, $R = 2 \times 10^{-2} \text{ cm}$, $\tau_{\text{pulse}} = 10^{-6} \text{ sec}$, and $r' = 10^{-8} \text{ sec}$.

We proceed to a discussion of the obtained solutions.

3. Figure 1 shows a calculated series of time scans of the electric field intensity at the sample (6) for different values of the current I_0 (these are exactly the relations determined directly in the experiment). An abrupt increase of the field intensity (to a value E_{max}) due to the rapid growth of the current (7) is followed by a decrease (to a value E_{min}) as a result of the avalanche-like growth of the number of particles through impact ionization (the conductivity increases). The field then increases again ($E = E_{\text{pinch}}$) and its subsequent value oscillates about a certain value $E_{\text{min}} < E_{\text{av}} < E_{\text{pinch}}$. The rise in the electric field intensity after reaching the value E_{min} is attributed^[10] to the onset of the pinch effect. Owing to the strong contraction of the plasma, the quadratic volume recombination processes become stronger in the contraction zone and lead to a decrease of the number of particles in the sample. The electron-hole scattering effects that decrease the electron mobility are also enhanced. These processes contribute to a decrease in the crystal conductivity. To confirm this assumption, we present time scans of the particle number U , of the sample conductivity $\sigma(\rho=1)$, and of the plasma concentration on the axis in the case $\alpha=0.01$. In the case of weak currents ($I_0=7$ A, Fig. 2a), the scans of $N(0, T)$ are shifted in phase relative to U and σ by π , i.e., the decrease of the conductivity at the instant of maximum contraction is due to a decrease of the number of particles in the sample (the scans retain their shape at $\alpha=0$ regardless of the current). For large currents ($I_0=18$ A, Fig. 2b), when the plasma concentration in the contraction zone is large, the relations are different: the scan of $\sigma(\rho=1)$ is shifted

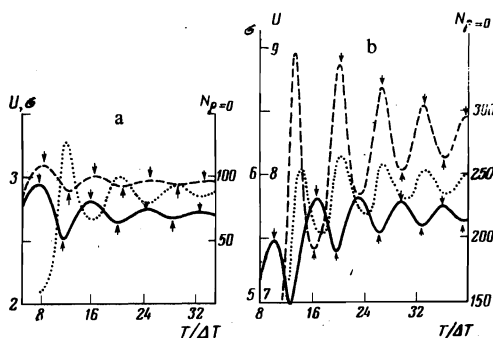


FIG. 2. Time scans of the plasma concentration on the sample axis $N_{\rho=0}$ (dotted curve), of the number of particles U (dashed), and of the sample conductivity σ (solid curve) at $I_0=7$ A (a) and 18 A (b). The parameters are $\gamma=0.128$; $\alpha=0.01$; $R^-=2$; $\Delta T=1/160$ (a) and $T=1/480$ (b).

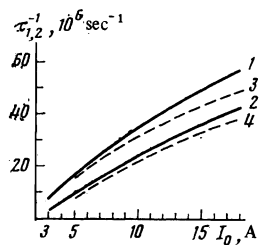


FIG. 3. Dependence of the pinch time on the current ($\gamma=0.128$, $R^-=2$). Curves 1 and 2— $\alpha=0.01$; 3 and 4— $\alpha=0.03$; τ_1 —pinch time determined from the plasma profile; τ_2 —pinch time determined from the time scan of the electric field intensity.

approximately by π relative to $N(0, T)$ and U . In this case the decrease of the conductivity during the pinch effect is due to electron-hole scattering. In the intermediate current interval $7 \text{ A} < I_0 < 18 \text{ A}$ the phase shift between U and σ varies from zero to π . We note that measurements of the corresponding phase shifts would make it possible to assess the role played by quadratic volume recombination and by electron-hole scattering under pinch-effect conditions.

The characteristic pinch time is usually^[10] defined as the time interval elapsed from the peak E_{max} to the first spike ($E = E_{\text{pinch}}$) connected with the appearance of the anomalous resistance (Fig. 1). The corresponding calculated plots of $\tau_2(I_0)$ are shown in Fig. 3 (curves 2 and 3) and agree with the experimental data.^[10] Figure 4b shows the radial profiles of the density at the instant of time when $E = E_{\text{pinch}}$, and attest to the strong contraction of the plasma. It should be noted that rather strong pinching takes place somewhat earlier; Fig. 4a shows the concentration distributions at the instants of time marked by the arrows in Fig. 1 (the plasma concentration on the sample axis is four times the average value at these instants). Figure 3 (curves 1 and 3) shows the corresponding plots of the pinch time $\tau_1(I_0)$ against the current. We note that for strong currents the effects of electron-hole scattering weaken the plasma contraction (the times τ_1 and τ_2 increase, see curves 3 and 4 of Fig. 3). It is more convenient to trace this tendency by investigating the dependence of the pinch radius ρ_{pinch} on the current. In analogy with the Bennet profile,^[11] $N = N(0, T)(1 + \rho^2/\rho_{\text{pinch}}^2)^{-2}$, we define the pinch radius as the point at which $N(0, T)/N(\rho = \rho_{\text{pinch}}, T) = 4$. The corresponding plots of $\rho_{\text{pinch}}(I_0)$

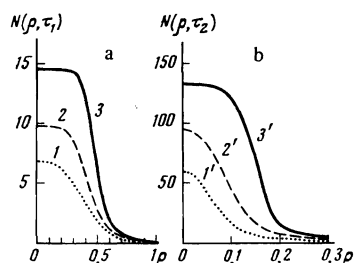


FIG. 4. Radial profiles of plasma density at the instants of time marked by arrows in Fig. 1(a) and at $E = E_{\text{pinch}}$ (b). Curve 1 (1')— $I_0 = 5 \text{ A}$; curve 2 (2')— $I_0 = 7 \text{ A}$; curve 3 (3')— $I_0 = 12 \text{ A}$; the parameters are $\gamma=0.128$; $\alpha=0.01$, and $R^-=2$.

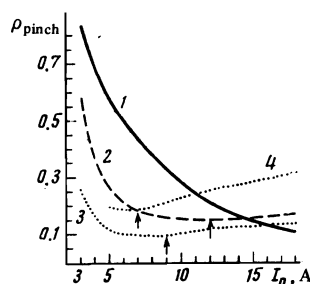


FIG. 5. Dependence of the pinch radius $N(0, T)/N(\rho = \rho_{\text{pinch}}, T) = 4$ on the current. 1— $\alpha=0$, $R^-=10$; 2— $\alpha=0.01$, $R^-=2$ ($\gamma=0.417$); 3— $\alpha=0.01$, 4— $\alpha=0.03$ ($\gamma=0.128$, $R^-=2$).

in Fig. 5 were calculated at the instants of time corresponding to establishment of the stationary state, when the oscillations of the field E are weakly pronounced. In the case when $\alpha=0$ (curve 1) the radius of the pinch decreases monotonically with the current. If $\alpha \neq 0$, then the corresponding plots are nonmonotonic (curves 2–4). At sufficiently large currents, when the plasma concentration is large, the electron-hole scattering weakens the radial flux and the pinch radius increases with the current (if $\alpha=0.01$, $R^-=2$, and $\gamma=0.417$, then a similar dependence sets in at $I_0 \approx 12 \text{ A}$ —curve 2; at $\alpha=0.005$, it sets in starting with $I_0 \approx 18 \text{ A}$). The arrows on Fig. 5 mark the currents at which this singularity in the behavior of $\rho_{\text{pinch}}(I_0)$ sets in. The results have made it possible to explain Morisaka's known experiments,^[7] where an increase of the pinch channel radius was observed in n -InSb at $I_0 = 20 \text{ A}$. As seen from Fig. 5, when the recombination, diffusion, and scattering parameters (R^- , γ , α) are increased, the pinch radius for a given current is increased.

Consider the behavior of the current-voltage characteristic for the pinch effect in n -InSb under impact ionization conditions (Fig. 6). If the recombination parameter is small (curves 2, 3, 4), so that the pinch effect is strong enough, the anomalies of the current-voltage characteristics are maximal, i.e., the deviation of the current-voltage characteristic from the reference (curve 1) is large. The reference current-voltage characteristic was plotted without allowance for the pinch effect (as if the sample were in a longitudinal magnetic field that destroys the pinch). Naturally, the current-voltage-characteristic anomalies,

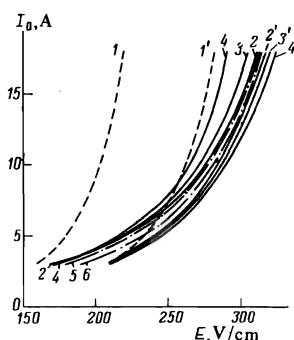


FIG. 6. Current-voltage characteristics of n -InSb samples in the pinch effect under impact-ionization conditions. Dashed curves (1. 1'— $\alpha=0.01$, $R^-=1$; 10)—references (plotted without allowance for the pinch effect); 2, 3, 4— $\alpha=0.01$; 0.04; 0.08 ($\gamma=0.417$; $R^-=1$); 2', 3', 4'— $\alpha=0.01$; 0.04; 0.08 ($\gamma=0.417$; $R^-=10$); 5, 6— $\gamma=0.417$; 0.128 ($\alpha=0.01$; $R^-=2$).

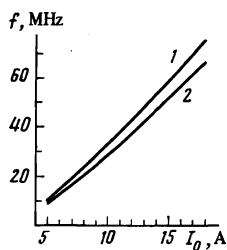


FIG. 7. Oscillation frequency vs current. Curves 1 and 2— $\alpha = 0.01$; 0.03 ($\gamma = 0.128$; $R^- = 2$).

which are due mainly to quadratic volume recombination, become weaker in this case (Fig. 6), inasmuch as the plasma contraction decreases (the reference curves differ little at the chosen values of α). If the recombination parameter is large (curves 2', 3', 4') the pinch effect becomes weaker and the deviation of the current-voltage characteristic from the reference (curve 1) is small. In this case the sequence of the current-voltage characteristics with increasing α is reversed. Variation of the parameter γ has a negligible effect on the current-voltage characteristic is the pinch is strongly developed (curves 5 and 6).

4. We now discuss the mechanism that governs the oscillatory character of the establishment of a stationary plasma state in n -InSb during the pinch effect. We present first the principal calculated data that characterize these oscillations. Figure 7 shows the dependence of the oscillation frequency on the current; it is close to linear, $f \sim I_0$. The experimental plots are similar to those obtained in [10, 12]. The small quantitative deviation from the experimental data (the calculated values are twice as large) is apparently due to the use of inexact parameters. The frequency decreases slightly with increasing α , R^- , and γ .

Figure 8 shows plots of the electric-field oscillation amplitude and of the damping coefficient (defined as the ratio of the amplitudes of neighboring maxima of the field E) against the current. It is clearly seen that when the parameters R^- , α , and γ are increased the oscillations become weaker. The damping coefficient increases also when these parameters are increased. We note that the function $E(I_0)$ at large values of α is nonmonotonic, i. e., the oscillations are produced in this case only in a definite current interval (curve 4). At lower values of α this nonmonotonicity is weaker and the oscillations values at large values of the current ($I_0 \approx 23$ A, curve 3). If $\alpha = 0$ then the oscillation amplitude always increases with increasing current (curve 1).

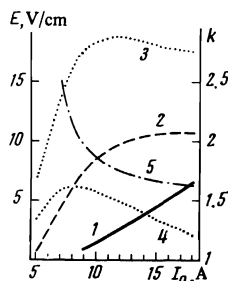


FIG. 8. Oscillation amplitude (curves 1 to 4— $E = (E_p - E'_{min})/2$, see Fig. 1) and damping coefficient k (5) vs current: 1— $\alpha = 0$, $R^- = 10$; 2— $\alpha = 0.01$, $R^- = 2$ ($\gamma = 0.417$); 3, 4— $\alpha = 0.01$; 0.03 ($\gamma = 0.128$, $R^- = 2$); 5— $\gamma = 0.128$, $\alpha = 0.01$, $R^- = 2$.

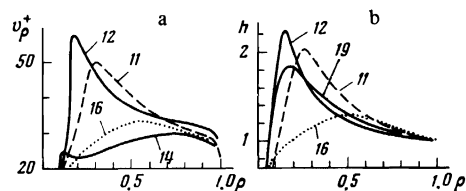


FIG. 9. Profiles of radial ambipolar hole drift velocity (a) and of the azimuthal magnetic current of the field ($h = H(\rho, T)/H(\rho = 1)$) at different instants of time for the variant shown in Fig. 1 (curve 3). The curves are tagged with the values of $T/\Delta T$.

We now examine the mechanism that gives rise to the pinch oscillations and explains, together with the results presented in Sec. 3, the obtained relations (Figs. 7 and 8).

When the pinch effect is strong it is possible to distinguish in the crystal two well-pronounced regions. In the first, located near the axis, the principal role is played by volume recombination and electron-hole scattering, while in the second (peripheral) impact ionization predominates. As the plasma contracts, the radial velocity of the holes ($v_r = v_p^+ R / \tau_{pulse}$, see Fig. 9a) in the peripheral region decreases at definite instant of time, owing to the shift of the maximum azimuthal magnetic field into the central region (Fig. 9b). During the evolution of the pinch, when the electric field on the sample increases, a plasma avalanche develops in the peripheral region, since its removal to the first region is hindered. As this avalanche develops, the conductivity of the crystal increases, and at a definite stage the azimuthal field and the radial drift velocity again increase in the peripheral region. Consequently the ionization wave produced on the periphery begins to move towards the center, and when it enters the region of strong contraction the crystal conductivity decreases. This process repeats periodically and attenuates in time.

When the current is increased, the pinch effect is more strongly pronounced and the effect of the blocking of the flux from the peripheral region is more noticeable; the ionization wave contains a large number of particles. Therefore the oscillation amplitude increases with increasing current. At large currents, when electron-hole scattering predominates in the central region (Fig. 2b), the pinch effect becomes weaker (Fig. 5, curves 2–4), the zones indicated above are less pronounced, and the ionization waves are much weaker (Fig. 8, curves 3 and 4). The oscillatory character of the time scans of the electric field intensity is due in fact to the strong pinching of the plasma. The absence of such oscillations is evidence of a weak pinch effect. We note that when comparing the previously discussed experimental data [10–12] it is necessary to assess attentively the role of the electron-hole scattering in these experiments, a role that depends on such parameters as the electron mobility (b_{e0}), the impurity density (n_0), the volume-recombination time, and others. These parameters could have been different in the different experiments, [10–12] and the picture of the pinch oscillations differs correspondingly.

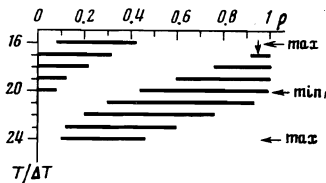


FIG. 10. Diagram illustrating the evolution of the ionization domain in space and time under pinch-effect conditions for the variant of Fig. 2a. The lines represent the crystal regions in which the plasma concentration is larger at a given instant of time (T) than in the preceding instant ($T - \Delta T$). The symbols max and min refer to extrema of the conductivity.

The damping of the oscillations in time can be explained in the following manner: Whereas the first field spike (Fig. 1, $E = E_{\text{pinch}}$) is due to contraction of practically all the carriers in the crystal, the succeeding spikes are due to the ionization wave generated on the periphery and delivering fewer particles to the contraction zone. The amplitude of the succeeding spikes therefore attenuates in time, since the amplitude of the ionization wave decreases gradually.

To calculate the oscillation frequency, we present a diagram (Fig. 10) that allows us to evaluate the evolution of the ionization wave in space and time. At the instant of time corresponding to the maximum of crystal conductivity ($\min E$) the ionization wave enters the pinch zone and the conductivity is decreased (the field increases). A new ionization wave (marked by a vertical arrow) is then produced immediately on the periphery. This wave increases gradually in space and "disengages" from the crystal surface at the instant $\sigma_{\rho=1} = \sigma_{\min}$. From this instant on, the sample conductivity increases. Prior to the next entry into the central zone ($\max \sigma$), the trailing edge of the wave is located at a distance $\rho \approx 0.5$. This picture (Fig. 10) changes little with changing current. We estimate the period of the oscillations defined as the time of ambipolar drift of a particle from the sample surface to the strong contraction zone. When estimating the ambipolar drift velocity we can neglect the diffusion and the electron-hole scattering. With the aid of (5) it is easy to obtain the following relation for the oscillation frequency:

$$f = \frac{4\pi b_0 b_{\infty}}{c^2} jE, \quad (12)$$

where j is the current density.

This expression agrees well with the results shown in Fig. 7 (curve 1). Since the field E varies little with current under impact ionization conditions (Fig. 6), the dependence of the oscillation frequency on the current is close to linear. According to (12), in thinner samples the oscillation frequency should increase ($\propto 1/R^2$). With increasing impurity density n_0 , the hole mobility can decrease^[21] and the oscillation frequency decrease, in agreement with the experimental data.^[10]

From the very meaning of the derivation of (12), the pinch time should coincide with the period of the oscillations. Indeed, from a comparison of the results shown in Figs. 7 we get $\tau_1 \approx 1/f$. A comparison with the experimental data^[10] confirms this conclusion.

We note finally that in the computer integration of Eqs. (9)–(11) we used a purely implicit difference scheme, the solution of which was obtained by an iteration method.^[22]

- ¹W. H. Bennett, Phys. Rev. **45**, 890 (1934); L. Tonks, Phys. Rev. **56**, 360 (1938).
- ²L. A. Artsimovich, Upravlyaemye termoyadernye reaktsii (Controlled Thermonuclear Reactions), Fizmatgiz, 1961 [Gordon, 1964].
- ³M. C. Steele and M. Glicksman, J. Phys. Chem. Solids **8**, 242 (1959); M. Glicksman and M. C. Steele, Phys. Rev. Lett. **2**, 461 (1959).
- ⁴B. V. Paranjape, J. Phys. Soc. Japan **22**, 144 (1967).
- ⁵E. Conwell and V. F. Weisskopf, Phys. Rev. **77**, 388 (1950).
- ⁶B. D. Osinov and A. N. Khovshchev, Zh. Eksp. Teor. Fiz. **43**, 1179 (1962) [Sov. Phys. JETP **16**, 833 (1963)]; M. Toda, Japan J. Appl. Phys. **2**, 467 (1963).
- ⁷H. Morisaki, J. Phys. Soc. Japan **32**, 736, 742 (1972).
- ⁸K. Ando and M. Glicksman, Phys. Rev. **154**, 316 (1967).
- ⁹Yu. L. Ivnov and S. M. Ryvkin, Zh. Tekh. Fiz. **28**, 774 (1958) [Sov. Phys. Tech. Phys. **3**, 722 (1958)]; B. B. Kadomtsev, A. V. Nedospasov, J. Nucl. En., Part C **1**, 230 (1960); M. Glicksman, Phys. Rev. **124**, 1655 (1961).
- ¹⁰M. Glicksman and R. A. Powlus, Phys. Rev. **121**, 1659 (1961); M. Glicksman, Proc. Seventh Intern. Conf. on Physics of Semiconductors, Paris, 1964, Vol. 2, Plasma Effects in Semiconductors, publ. by Dunod, Paris; Academic Press, New York (1965), p. 149.
- ¹¹A. G. Chynoweth and A. A. Murray, Phys. Rev. **123**, 515 (1961).
- ¹²M. Tacano and S. Kataoka, Jap. J. Appl. Phys. **14**, 261 (1975).
- ¹³J. E. Drummond and B. Aucker-Johnson, Proc. Seventh Intern. Conf. on Physics of Semiconductors, Paris, 1964, Vol. 2, Plasma Effects in Semiconductors, publ. by Dunod, Paris; Academic Press, New York (1965), p. 173.
- ¹⁴Yu. L. Igitkhanov, Zh. Eksp. Teor. Fiz. **56**, 1619 (1969) [Sov. Phys. JETP **29**, 867 (1969)]; Yu. L. Igitkhanov and B. B. Kadomtsev, Zh. Eksp. Teor. Fiz. **59**, 155 (1970) [Sov. Phys. JETP **32**, 86 (1971)].
- ¹⁵W. S. Chen and B. Ancker-Johnson, Phys. Rev. **B2**, 4468 (1970).
- ¹⁶M. A. Leontovich and S. M. Osovets, At. Energy. **3**, 81 (1956); B. F. Niblett and T. S. Green, Proc. Phys. Soc. Lond. **74**, 737 (1959).
- ¹⁷Ø. Holter, Phys. Rev. **129**, 2548 (1963).
- ¹⁸Y. Marechal, J. Phys. Chem. Solids **25**, 401 (1964).
- ¹⁹M. C. Steele and S. Toshima, Japan J. Appl. Phys. **2**, 381 (1963).
- ²⁰J. C. McGroddy and M. J. Nathan, J. Phys. Soc. Japan, Suppl. **21**, 437 (1966).
- ²¹G. Busch and E. Steigmeier, Helv. Phys. Acta **34**, 1 (1961).
- ²²A. A. Samarskii, Vvedenie v teoriyu raznostnykh akhem (Introduction to the Theory of Difference Schemes), Nauka, 1971, p. 214.

Translated by J. G. Adashko